Taylor & Francis
Taylor & Francis Group

Molecular Crystals and Liquid Crystals

ISSN: 1542-1406 (Print) 1563-5287 (Online) Journal homepage: http://www.tandfonline.com/loi/gmcl20

TPCO single-crystal optical devices equipped with one-dimensional diffraction gratings

Kazuki Aoki, Yuki Obama, Satoru Sugimoto, Takeshi Yamao & Shu Hotta

To cite this article: Kazuki Aoki, Yuki Obama, Satoru Sugimoto, Takeshi Yamao & Shu Hotta (2016) TPCO single-crystal optical devices equipped with one-dimensional diffraction gratings, Molecular Crystals and Liquid Crystals, 636:1, 45-51, DOI: 10.1080/15421406.2016.1200942

To link to this article: http://dx.doi.org/10.1080/15421406.2016.1200942

MOLECULAR CRYSTALS AND LIQUID CRYSTALS
2016, VOL. 636, 45–51
http://dx.doi.org/10.1080/15421406.2016.1200942

Taylor & Francis
Taylor & Francis Group

TPCO single-crystal optical devices equipped with one-dimensional diffraction gratings

Kazuki Aoki, Yuki Obama, Satoru Sugimoto, Takeshi Yamao, and Shu Hotta

Faculty of Materials Science and Engineering, Kyoto Institute of Technology, Matsugasaki, Sakyo-ku, Kyoto, Japan

ABSTRACT

We have formed one-dimensional (1D) diffraction gratings on a photoresist polymer (SU-8) by interference exposure using a Lloyd mirror. A single crystal of thiophene/phenylene co-oligomers (TPCOs) grown in a vapor phase was placed on the 1D diffraction grating. Excitation of the single crystal by an ultraviolet light of a mercury lamp produced spectrally-narrowed fluorescence. On the basis of the grating periods and emission peak locations, we evaluated effective refractive indices and diffraction orders. The relevant information enables us to design and fabricate the 1D diffraction gratings that cause the spectrally-narrowed emission lines to superimpose inherently occurring high-intensity fluorescence peaks.

KEYWORDS

Diffraction grating; thiophene/phenylene co-oligomers; single-crystal devices

Introduction

Organic semiconductor single-crystals generally combine high carrier mobility and fluorescence efficiency. These crystals also exhibit laser oscillation and related spectrally-narrowed emissions (SNEs) [1–6]. If the crystals are equipped with a suitable optical grating, the resulting structure can directly be used for a unique optoelectronic device. To construct a high-performance optical device, detailed information on optical constants (e.g. refractive indices) should be available with individual chemical species of crystals. In this respect we have already developed a simple but effective method to determine the refractive indices of organic single crystals [7–9]. The method is based upon careful observation and measurements of optical fringes that take place in emission spectra. In that case a pair of parallel crystal facets at both ends functions as a Fabry-Pérot resonator. For most of optical device applications of the single crystals, however, the crystals act as a waveguide. In this case we are dealing with an *effective* refractive index instead of a *phase* refractive index.

Within a framework of determining the effective refractive index, we made one-dimensional (1D) diffraction gratings of different grating periods on a photoresist polymer (SU-8) by interference exposure using a Lloyd mirror. On the diffraction grating we placed a single crystal of thiophene/phenylene co-oligomers (TPCOs) to construct an optical device. In the present studies we chose BP3T and P6T [see Fig. 1(a) for structural formulae] from among various TPCOs [10,11]. Excitation of the single crystal by ultraviolet light of a mercury lamp produced angle-dependent spectrally-narrowed fluorescence. On the basis of the

CONTACT Shu Hotta hotta@kit.ac.jp Faculty of Materials Science and Engineering, Kyoto Institute of Technology, Matsugasaki, Sakyo-ku, Kyoto 606-8585, Japan.
Color versions of one or more of the figures in the article can be found online at www.tandfonline.com/gmcl.

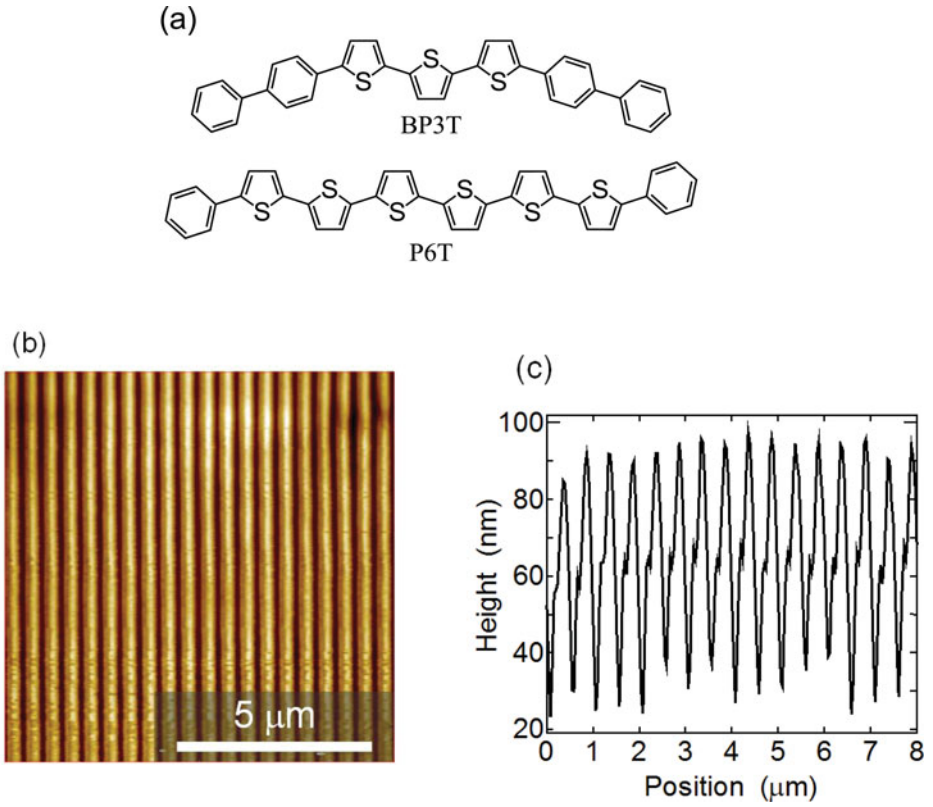

Figure 1. (a) Structural formulae of BP3T and P6T. (b) AFM image of a SU-8 diffraction grating. (c) Surface and depth profile of the diffraction grating of (b).

experimental results on emission data obtained from various single crystal waveguides having different grating periods and emission peak locations, we evaluated effective refractive indices and diffraction orders of the waveguides. Crystal thicknesses play a role as well. Finally, we propose a practical guideline to design a high-performance optical device.

Experiments

Photoresist films were spin-coated from either a solution of MicroChem SU-8 2000.5 polymer without dilution or a 12.5 wt% cyclopentanone solution of a MicroChem SU-8 3005 polymer on a silicon dioxide layer (300 nm in thickness) which was formed on top of a quarried 1-cm square silicon wafer. The resulting photoresist film was baked to evaporate the solvent (first at 65°C for 15 min and subsequently at 95°C for 15 min). To form the diffraction grating on the photoresist film, we carried out the interference exposure to that film using a Lloyd mirror as before [12–14]. We used for an exposure source third harmonic generation of an Nd:YAG laser (wavelength: 355 nm, pulse duration: 25 ps, repetition rate: 10 Hz). After the laser beam exposure we baked the photoresist film to ensure the curing reaction (at 65°C for 10 min and subsequently at 95°C for 10 min). The film was then developed, rinsed with 2-propanol, and dried. We further baked the film at 175°C for 20 min to complete the reaction. We set the angle of the Lloyd mirror at 20.0° to 27.0° from the direction normal to the film surface. As a result, we obtained diffraction gratings whose periods ranged from 394.0 to 498.6 nm. We observed a surface of the diffraction grating with a Pacific Nanotechnology Nano-R^{TM} atomic

Table 1. Characterization of crystal samples and diffraction gratings.

Sample	Lloyd mirror angle (degree)	Crystal thickness *d* (nm)	Grating period Λ (nm)	Depth of Grooves (nm)
P6T-1	24.7	491	427.8	36.6
P6T-2	22.0	120	463.4	54.1
P6T-3	22.0	461	464.4	54.5
P6T-4	22.0	635	468.8	49.4
P6T-5	22.0	1249	467.1	53.2
P6T-6	21.9	233	478.1	87.4
BP3T-1	20.0	493	498.6	61.8
BP3T-2	22.0	338	476.4	52.5
BP3T-3	22.0	393	480.6	58.0
BP3T-4	22.5	345	444.7	69.8
BP3T-5	22.5	258	461.1	72.8
BP3T-6	27.0	394	394.0	38.5

force microscope (AFM). Figure 1(b) shows an example of its micrograph for a specific sample of BP3T-1 (see Table 1). Figure 1(c) shows a depth profile of this diffraction grating.

We made single crystals of BP3T and P6T by a vapor phase recrystallization method. Detailed setup of apparatus and crystal growth procedures can be seen elsewhere [15,16]. We measured crystal thicknesses using a BRUKER Dektak XT stylus profiler. Table 1 collects characteristic angles and dimensions of different samples. We measured emission spectra from single crystals using an experimental setup and measurement geometry same as before [17]; an excitation ultraviolet light was incident to a wide crystal plane of the sample. The emission spectra were collected in a direction parallel to the crystal plane as a function of angles of rotation about the axis normal to the crystal plane. The rotation angle was defined as an angle made by the emission direction and that of the grating wave vector. It was defined as positive when the sample was rotated counterclockwise. In this geometry, we measured the emission spectra from −90 to +90° in 5° to 10° steps.

Results and discussion

Figure 2 shows angle-dependent spectra of P6T-1 and BP3T-1 samples. For both the spectra we observed two series of major emission lines progressively redshifted relative to that taken at a rotation angle $\theta = 0°$. We assume the Bragg reflection with the emission observed at $\theta = 0°$

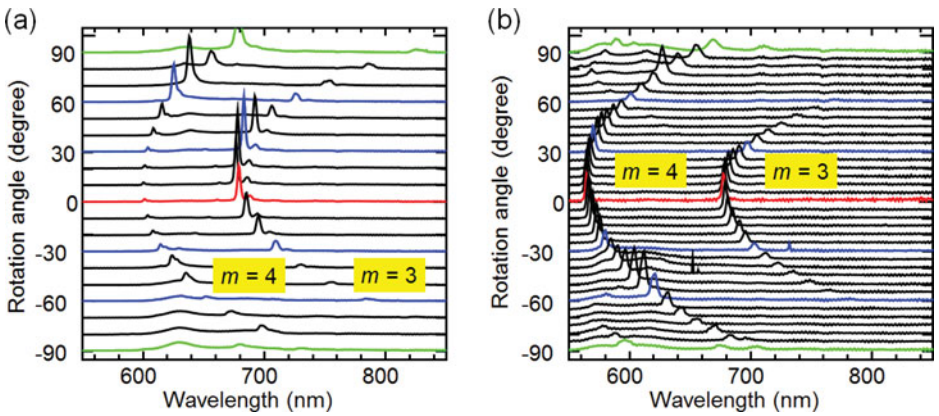

Figure 2. (a) Angle-dependent spectra of P6T-1. (b) Angle-dependent spectra of BP3T-1. The indices *m* denote the diffraction order.

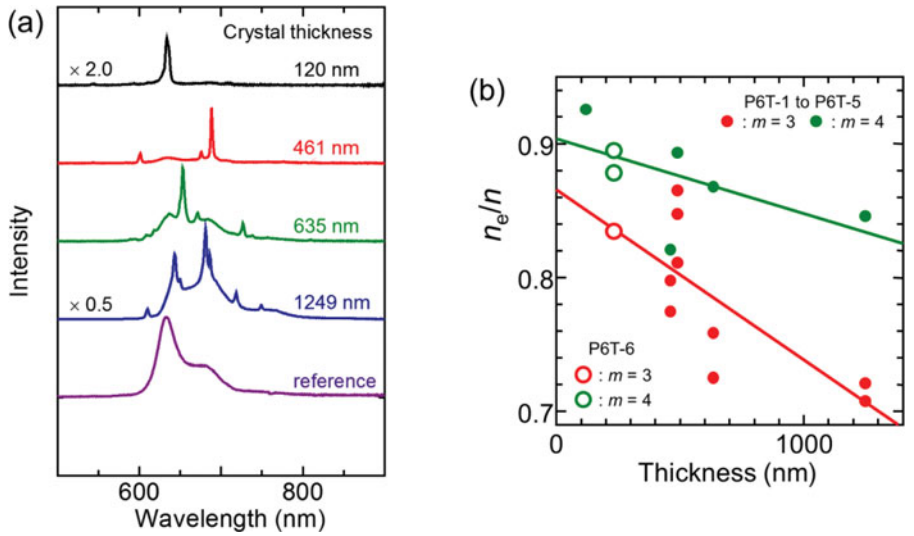

Figure 3. (a) Emission spectra taken at the rotation angle $\theta = 0°$ as a function of crystal thicknesses. (b) Relationship between the n_e/n ratio and crystal thicknesses. The least-squares lines were determined from the plots for the diffraction order $m = 3$ or $m = 4$ individually using PT6-1 to PT6-5 with different crystal thicknesses.

among the series of spectra as follows [18,19]:

$$m\lambda = 2n_e\Lambda, \tag{1}$$

where m is a diffraction order, $\lambda$is the emission peak wavelength measured at $\theta = 0°$, n_e is the effective refractive index, and Λ is the grating period. We determined m and n_e in such a way that n_e did not exceed a phase refractive index n at λ in question and m was the maximum integer on this condition. Here we assume Sellmeier dispersion relationship between n and λ [20,21]. As a result we assign individual redshifted progressions to a specific number of m as shown in Fig. 2. Note that we obtained related results with BP3T crystals.

Next we compared spectral profiles of various crystals of different thicknesses. Figure 3(a) shows the results of P6T crystals. We notice the following trends from Fig. 3(a): (i) The larger number of emission lines was observed with increasing crystal thicknesses. Crystals of a few hundred micrometers gave distinctly narrowed emission lines. (ii) Broadband spectra became easier to notice near ~630 and ~680 nm with increasing crystal thicknesses. These bands are generally accompanied by large optical gains. We also examined the dependence of crystal thickness on refractive index. As an example Fig. 3(b) depicts the results of P6T crystals using PT6-1 to PT6-5 with different crystal thicknesses (see Table 1). Two lines in the diagram are least-squares lines determined from the plots for $m = 3$ or $m = 4$ individually. The ratio of n_e to n (n_e/n) tends to decreases with increasing crystal thicknesses.

This can reasonably be explained by the following argument: Viewing the crystals of P6T and BP3T as a slab waveguide, the presence of both the top and bottom wide crystal planes imposed boundary conditions on propagation of electromagnetic waves within the waveguide (i.e. transverse modes). Defining k_2 as a component of the wavenumber vector ($\boldsymbol{k}$) parallel to the normal of the slab plane, $|\boldsymbol{k}|^2 = {k_1}^2 + {k_2}^2$, where $k_1 = 2\pi n_e/\lambda = m\pi/\Lambda$ is a component of the wavenumber vector parallel to the slab plane [22]. The boundary conditions require $k_2 = l\pi/d$, where l is the order of the transverse mode (a positive integer) and d is the crystal

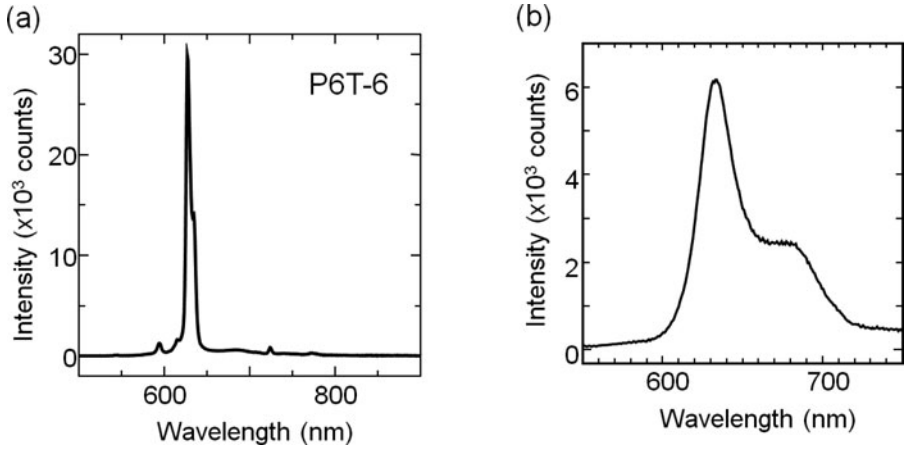

Figure 4. (a) Emission spectra of P6T-6 taken at the rotation angle $\theta = 0°$. (b) Emission spectra of a P6T crystal without a diffraction grating.

thickness. Combining these relationships with Eq. (1), we obtain the following expression:

$$\frac{n_e}{n} = \sqrt{\frac{1}{1 + (l^2 \Lambda^2 / d^2 m^2)}}. \tag{2}$$

The implications of Eq. (2) are as follows: (i) Larger numbers of m give larger numbers of n_e/n. (ii) If the number m is small, the variation in n_e/n is more conspicuous with varying numbers of l and Λ. These trends are consistent with experimental data represented in Fig. 3(b). More specifically, compared to a larger number of m ($m = 4$ in the present case) a smaller number of m ($m = 3$ in the present case) produces a relatively large deviation of n_e/n from the least-squares line as indicated in Fig. 3(b). Equations (1 and 2) as well as Fig. 3(b) give us a practical guideline to design a single-crystal optical device. These relationships have enabled us to design a device with an optimum grating period so that it can produce a narrowed and strong emission line at $\theta = 0°$ and around a specific emission band at which a large optical gain is anticipated (e.g. ~630 and 680 nm for P6T). In a word, we become able to determine an optimum grating period Λ at an aimed emission wavelength λ.

Thus we finally made P6T-6 with the crystal thickness of 233 nm (Table 1). As represented in Fig. 4(a), we observed a dominant narrowed emission line at 627.3 nm ($\theta = 0°$) with a full width at half maxima (FWHM) of 4.5 nm [Fig. 4(a)] with this specific device. The n_e/n number estimated from Eq. (2) was 0.89 for $m = 4$ with $l = 1$. This is in excellent agreement with the experimentally determined number (0.88 for $m = 4$). This result should be compared to that for a P6T crystal without a diffraction grating [Fig. 4(b)]. The emission intensity of P6T-6 was about five times as strong as that of Fig. 4(b). We emphasize that it will of great importance from a practical point of view to cause the spectrally-narrowed emission lines to superimpose the high-intensity fluorescence peaks that are accompanied by an inherently large optical gain. In fact, the emission line occurring at $\theta = 20°$ (around 680 nm) for the series of spectra assigned to $m = 3$ along with that noticed at $\theta = 70°$ (around 630 nm) for those assigned to $m = 4$ indicated enhanced intensities [see Fig. 2(a)]. If this is the case with $\theta = 0°$, optical amplification should be anticipated.

We obtained similar results with BP3T devices. Figure 5 compare the results obtained from BP3T-6 and a BP3T crystal without a diffraction grating. Since the latter crystal (without

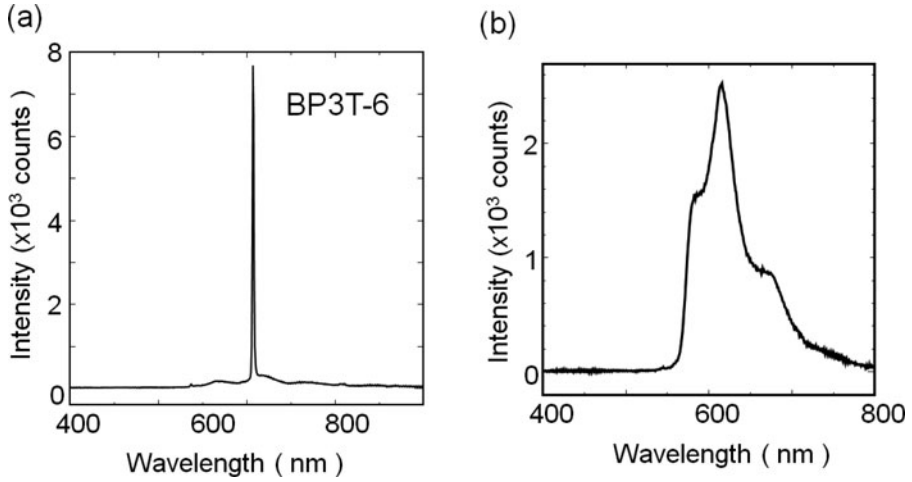

Figure 5. (a) Emission spectra of BP3T-6 taken at the rotation angle $\theta = 0°$. (b) Emission spectra of a BP3T crystal without a diffraction grating.

grating) exhibited a strong band at 616 nm, we designed an optimum BP3T device (BP3T-6) as in the case of P6T devices. This specific device showed a narrowed line at 608.0 nm ($\theta = 0°$) with FWHM of 2.0 nm; see Fig. 5(a). Again the emission intensity of BP3T-6 was about three times as strong as that of Fig. 5(b) that shows a spectrum of a BP3T crystal without a diffraction grating.

Conclusions

We have made single-crystal optical devices equipped with a 1D diffraction grating. The gratings were formed on a photoresist polymer (SU-8) by interference exposure using a Lloyd mirror. A single crystal of thiophene/phenylene co-oligomers (TPCOs) grown in a vapor phase was placed on the diffraction grating. Excitation of the single crystal by an ultraviolet light of a mercury lamp produced spectrally-narrowed emissions. Peak locations of the major emission lines exhibited angle-dependent redshifts relative to the grating wave vector direction. We assumed the Bragg reflection at the rotation angle $\theta = 0°$ in the progressively redshifted spectra. Collecting emission data on the gratings with various periods, we have determined the diffraction orders and effective refractive indices. Taking account of different crystal thicknesses, we also sought the relationship between the crystal thicknesses and the ratios of effective refractive indices to phase refractive indices.

These experimental results and numerical analyses have enabled us to determine an optimum grating period Λ at an aimed emission wavelength λ with an appropriate combination of a diffraction order m and mode order of l. In particular, we can readily cause a narrowed emission line to superimpose a specific emission band accompanied by an inherently large optical gain. This feature will be a powerful practical guideline to design a high-performance optical device.

Acknowledgments

This work was supported by Grants-in-Aid for Scientific Research A (Grant No. 25248045) and Challenging Exploratory Research (Grant No. 24655173) from Japan Society for the Promotion of Science (JSPS).

References

[1] Ichikawa, M., Hibino, R., Inoue, M., Haritani, T., Hotta, S., Araki, K., Koyama, T., & Taniguchi, Y. (2005). *Adv. Mater.*, *17*, 2073.
[2] Ichikawa, M., Nakamura, K., Inoue, M., Mishima, H., Haritani, T., Hibino, R., Koyama, T., & Taniguchi, Y. (2005). *Appl. Phys. Lett.*, *87*, 221113.
[3] Shimizu, K., Mori, Y., & Hotta, S. (2006). *J. Appl. Phys.*, *99*, 063505.
[4] Yamao, T., Yamamoto, K., Taniguchi, Y., Miki, T., & Hotta, S. (2008). *J. Appl. Phys.*, *103*, 093115.
[5] Mizuno, H., Ohnishi, I., Yanagi, H., Sasaki, F., & Hotta, S. (2012). *Adv. Mater.*, *24*, 2404.
[6] Holmes, R. J. (2007). *Nat. Nanotechnol.*, *2*, 141.
[7] Yamao, T., Taniguchi, Y., Yamamoto, K., Miki, T., Ota, S., Hotta, S., Goto, M., & Azumi, R. (2007). *Jpn. J. Appl. Phys.*, *46*, 7478.
[8] Yamao, T., Okuda, Y., Makino, Y., & Hotta, S. (2011). *J. Appl. Phys.*, *110*, 053113.
[9] Sugimoto, S., Fukunishi, Y., Fukaya, Y., Yamao, T., & Hotta, S. (2013). *Trans. Mat. Res. Soc. Japan*, *38*, 301.
[10] Hotta, S., Kimura, H., Lee, S. A., & Tamaki, T. (2000). *J. Heterocycl. Chem.*, *37*, 281.
[11] Hotta, S., & Katagiri, T. (2003). *J. Heterocycl. Chem.*, *40*, 845.
[12] Kranzelbinder, G., Toussaere, E., Zyss, J., Pogantsch, A., List, E. W. J., Tillmann, H., & Hörhold, H.-H. (2002). *Appl. Phys. Lett.*, *80*, 716.
[13] Tsutsumi, N., & Fujihara, A. (2005). *Appl. Phys. Lett.*, *86*, 061101.
[14] Makino, Y., Hinode, T., Okada, A., Yamao, T., Tsutsumi, N., & Hotta, S. (2011). *Phys. Procedia*, *14*, 177.
[15] Yamao, T., Ota, S., Miki, T., Hotta, S., & Azumi, R. (2008). *Thin Solid Films*, *516*, 2527.
[16] Fukaya, Y., Inoue, A., Fukunishi, Y., Hotta, S., & Yamao, T. (2013). *Jpn. J. Appl. Phys.*, *52*, 05DC09.
[17] Fukaya, Y., Obama, Y., Hotta, S., & Yamao, T. (2014). *Jpn. J. Appl. Phys.*, *53*, 01AD08.
[18] Schneider, D., Hartmann, S., Benstem, T., Dobbertin, T., Heithecker, D., Metzdorf, D., Becker, E., Riedl, T., Johannes, H. H., Kowalsky, W., Weimann, T., Wang, J., & Hinze, P. (2003). *Appl Phys B*, *77*, 399.
[19] Samuel, I. D. W., & Turnbull, G. A. (2007). *Chem. Rev.*, *107*, 1272.
[20] Smith, F. G., King, T. A., & Wilkins, D. (2007). *Optics and Photonics: An Introduction*, Wiley: Chichester, UK.
[21] Born, M., & Wolf, E. (1999). *Principles of Optics: Electromagnetic Theory of Propagation, Interference and Diffraction of Light*, Cambridge University Press: Cambridge, UK.
[22] Pain, H. J. (1999). *The Physics of Vibrations and Waves*, Wiley: Chichester, UK.